Effect of Organic Modifiers and Silicate Type on Filler Dispersion, Thermal, and Mechanical Properties of ABS-Clay Nanocomposites

Rajkiran R. Tiwari, Upendra Natarajan

Division of Polymer Science and Engineering, National Chemical Laboratory, Pune 411008, India

Received 18 September 2007; accepted 6 May 2008
DOI 10.1002/app.28699
Published online 20 August 2008 in Wiley InterScience (www.interscience.wiley.com).

ABSTRACT: Acrylonitrile–butadiene–styrene (ABS)–clay composite and intercalated nanocomposites were prepared by melt processing, using Na-montmorillonite (MMT), several chemically different organically modified MMT (OMMT) and Na-laponite clays. The polymer–clay hybrids were characterized by WAXD, TEM, DSC, TGA, tensile, and impact tests. Intercalated nanocomposites are formed with organoclays, a composite is obtained with unmodified MMT, and the nanocomposite based on synthetic laponite is almost exfoliated. An unintercalated nanocomposite is formed by one of the organically modified clays, with similar overall stack dispersion as compared to the intercalated nanocomposites. T_g of ABS is unaffected by incorporation of the silicate filler in its matrix upto 4 wt % loading for different aspect ratios and organic modifications. A significant improvement in the onset of thermal decomposition (40–44°C at 4 wt % organoclay) is seen. The Young's modulus shows improvement, the elongation-at-break shows reduction, and the tensile strength shows improvement. Notched and unnotched impact strength of the intercalated MMT nanocomposites is lower as compared to that of ABS matrix. However, laponite and overexchanged organomontmorillonite clay lead to improvement in ductility. For the MMT clays, the Young's modulus (E) correlates with the intercalation change in organoclay interlayer separation (Δd_{001}) as influenced by the chemistry of the modifier. Although ABS-laponite composites are exfoliated, the intercalated OMMT-based nanocomposites show greater improvement in modulus. © 2008 Wiley Periodicals, Inc. J Appl Polym Sci 110: 2374–2383, 2008

Key words: styrene–butadiene; clay; filler; mechanical; structure characterization

INTRODUCTION

Polymer–clay nanocomposites are hybrid materials with heterogeneity in chemical structure as well as physical properties because of reinforcements over nanometer length scales.[1,2] Such materials are known to show significant improvement in thermal and mechanical properties usually obtained at low fraction of clay.[3] Clay-based nanocomposites exhibit tremendous improvements in tensile strength,[4] modulus,[4,5] barrier to permeation of small molecules,[6] and fire retardancy.[7] Acrylonitrile–butadiene–styrene (ABS) copolymers are widely used commercially as engineering thermoplastics, known to exhibit excellent toughness and good dimensional stability. Grafting of styrene–acrylonitrile copolymer onto butadiene elastomeric polymer backbone, to give a distinct rubber phase in a sufficiently compatible manner with the glassy styrene–acrylonitrile phase, is the usual way ABS copolymers are prepared.[8] Commercial ABS resins are compatible (miscible) blends of graft ABS copolymer and styrene–acrylonitrile random copolymer. The most desired properties in applications are their toughness and dimensional stability. Desired property enhancements for ABS include better or improved tensile strength and modulus, heat deflection temperature, and thermal expansion coefficients, preferably without loss of its inherent ductility.

Melt processing of thermoplastic polymers with clay is a viable and chemically convenient method for preparation of nanocomposites. A variety of engineering thermoplastics, such as polyethylene (PE),[9,10] polypropylene,[10] nylon 6,[11] PMMA, polystyrene (PS),[13] polycarbonate[14] among others, have been investigated by the melt-mixing method. Existing literature on preparation and properties of ABS-clay nanocomposites[15–27] discusses in situ polymerization and melt-processing methods that have been employed; however, results on mechanical properties and of melt-processed nanocomposites are scarce. There is a need for a detailed study to understand the effect of chemical structure of the organic

Correspondence to: U. Natarajan (upen.natarajan@gmail.com or u.natarajan@ncl.res.in).

Contract grant sponsor: Council of Scientific and Industrial Research, India.

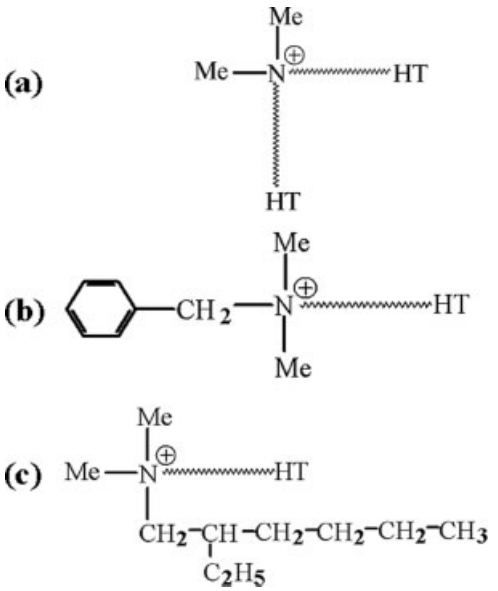

Figure 1 Chemical structures of the quaternary ammonium modifiers: (a) dimethyl dihydrogenated tallow quaternary ammonium used in Cloisite® 6A and Cloisite® 20A, (b) dimethyl benzyl hydrogenated tallow quaternary ammonium used in Cloisite® 10A, and (c) dimethyl hydrogenated tallow 2-ethylhexyl quaternary ammonium used in Cloisite® 25A.

modifier and its platelet size on the thermal stability and mechanical properties of ABS hybrids. This is a first report to our knowledge on the properties of ABS-clay composites and nanocomposites as affected by differences in the type of clay filler (i.e., montmorillonite (MMT) and laponite). Laponite systems have not been explored at all with ABS as a potential nanocomposite matrix. Some of the organic modifier molecules which are studied here [in Cloisite 25A, Cloisite 20A, and Cloisite 10A organically modified montmorillonite (OMMTs)] have been looked at in a recent report in the literature,[27] which had focused on differences in the behavior of SAN and ABS matrices toward interaction with certain types of alkylammonium modifiers. While the results of our present study conducted under different processing conditions and polymer grade as compared to the previous report are quite similar,[27] the newer results using different clays and synthetic clay laponite (as a function of clay loading in nanocomposite) are brought forth additionally. The influence of the organic modifiers on the thermal (glass transition, stability, and degradation) and mechanical (Young's modulus, properties at failure, impact strength) properties of these nanocomposites are presented here. For two types of organoclays, the effect of clay loading on the extent of intercalation and the improvement in the modulus is shown and rationalized here.

EXPERIMENTAL

Materials

ABS polymer resin (Absolac120) extrusion and injection molding grade with an acrylonitrile content of 23 wt % was supplied by Bayer ABS Ltd., Vadodara, India. The commercial ABS samples used in this study contain low butadiene content and stabilizers in very small amounts to prevent chain degradation during extrusion and injection molding. The melt flow index of ABS was determined as 1.5 g/10 min using 2.16 kg load cell at 180°C. Sodium montmorillonite along with four different commercially available OMMTs, and Laponite nanoclay were supplied by Southern Clay Products Inc. (Gonzales, TX). The organomontmorillonite contains different organic modifiers in terms of hydrophobicity, structure, and molecular weight. Na-laponite unmodified clay is laponite-RD grade from Laporte Industries Ltd. (Widnes, UK). The chemical formula is $Na_{0.7}^{+}[(Si_8Mg_{5.5}Li_{0.3})O_{20}(OH)_4]^{-0.7}$, with each platelet having a diameter of 30 nm and a thickness of 1 nm, and a cation exchange capacity (CEC) of 70 mequiv/100 g. The chemical structures of organic modifier are shown in Figure 1. The details of the organic modifiers, CEC and *d*-spacing of the clays, are provided in Table I.

Nanocomposite preparation

ABS resin pellets and clay powder samples were dried in a vacuum oven at 80°C for 12 h prior to the

TABLE I
Specifications and Organic Modifications of Clays

Clay	Quaternary ammonium ion	CEC/ loading[a]	*d*-spacing (nm)
Cloisite® Na^+ (CNa)	–	92.6	1.21
Cloisite® 10A (C10A)	Dimethyl benzyl hydrogenated tallow	95	1.92
Cloisite® 6A (C6A)	Dimethyl dihydrogenated tallow	140	3.54
Cloisite® 20A (C20A)	Dimethyl dihydrogenated tallow	95	2.42
Cloisite® 25A (C25A)	Dimethyl hydrogenated tallow 2-ethylhexyl	95	1.86
Laponite-RD®	–	70	1.23

[a] CEC for Na^+MMT and Na^+laponite while organic loading values are for organoclay in mequiv/100 g.

mixing/processing experiments. The mixture of ABS and clay was extruded through Berstoff ZE-25 corotating twin-screw extruder (Hannover, Germany) (diameter = 25 mm, $L/D = 40$) operated in a continuous mode. The temperature of heating zones was varied uniformly as feed = 180°C, cylinder temperature was varied from 185 to 190°C, and die temperature 210°C, based on standard conditions for processing of ABS.[8] The screws speed was kept at 100 rpm for all runs. Purging was done using standard PE grades as well as ABS. The extruded samples were then pelletized to uniform standard size using a pelletizer. Films for WAXD characterization were prepared by compression molding in a Carver® press at 160°C for 10 min under the pressure of 4 MPa.

Samples for study as a function of clay loading (range 2–10 wt % inclusive of organic content on MMT) were prepared in a Haake Rheocord internal batch mixer (Waltham, MA) (capacity $\sim$ 51cm^3). This study was carried out for organoclays C20A, C25A (each having different organic modifier and architecture) and laponite. Mixing was done at 180°C for 15 min at a mixing speed of 60 rpm, which was found to be satisfactory based on our optimization experiments; also similar to systems based on PS and PMMA.[12]

Structure characterization

WAXD was performed on at least three multiple films from each system to ascertain the correct data. The variation of the *d*-spacing results for all systems was found to be within the acceptable limit of experimental error. The WAXD patterns were recorded on a Rigaku diffractometer (Tokyo, Japan) using Cu Kα radiation ($\lambda = 0.15418$ nm) at 50 kV and 120 mA. The experiments were performed in a scan range of $2\theta = 2$–15° with a scan speed of 1°/min on compression-molded film. This condition gives smooth curves that are accurate for nanocomposites in terms of the identification of peak positions and establishing the scattering behavior.

Bright-field TEM images of the nanocomposites were obtained at an accelerating voltage of 80 kV using a JEOL 1200EX transmission electron microscope (Tokyo, Japan). For MMT-based hybrids, $\sim$ 50–70 nm sections were microtomed with a diamond knife using Leica Ultracut UCT microtome (Vienna, Austria). The sections were collected on 300-mesh carbon-coated copper grids from water boat. The copper grids were dried on filter paper. The density of the clay particles is sufficient to get contrast between polymer and clay stacks, hence staining for the sections was not required. Images were captured using a charge coupled detector camera and further analyzed (including quantitative analysis of clay platelet/stack lengths) using Gatan Digital Micrograph analysis software (Warrendale, PA).

The stacks statistics were obtained based on 200–250 counts from seven or more different images for each of the organomontmorillonite-based ABS nanocomposites. For the laponite nanocomposite, the clay stack distribution and size measurements are based on TEM images obtained from a 100-nm thin section, as it was not possible to obtain proper sections at less than 100 nm thickness at room temperature. The statistics were obtained using 189 counts from several (nine) images, to calculate the mean particle length of the uniformly dispersed laponite clay stacks.

Thermal analysis

The thermal properties of the ABS hybrids were measured by TA Instruments (New Castle, DE) Q10 differential scanning calorimeter under standard conditions. The measurements were done in the temperature range of 50–180°C because of the dominant styrene-*co*-acrylonitrile segments of ABS, as we are not specifically interested in the very low temperature relaxation from the butadiene segments in the present study. Typically, a sample of about 3–4 mg was heated first from 50 to 180°C at a heating rate of 10°C/min to relieve any thermal history of the glassy state. The sample was allowed to cool to 50°C at the rate of 50°C/min and subsequently reheated from 50 to 180°C. The data obtained from the second scan was used to determine the glass transition temperature of the ABS and its hybrids. DSC results clearly showed occurrence of glass transition temperature for the ABS and its hybrids.

TGA measurements were carried out on Perkin–Elmer TGA-7 (Waltham, MA). Sample $\sim$ 4–7 mg was heated from 50 to 700°C at rate 10°C/min under nitrogen atmosphere. Same heating rates were used for ABS and the composite samples. The final amount of mass left at 700°C was proportional to the amount of inorganic content in each of the hybrids (for samples where total organoclay content was fixed at 4 wt %), which was different for each hybrid due to different amounts of organic modifier mass per gram of MMT.

Mechanical tests

For the samples prepared using Berstoff ZE-25 corotating twin-screw extruder, the dumbbell shape specimens for tensile testing (ASTM D 638) and impact specimens (ASTM D 256) were injection molded on Arburg® all-rounder injection molding machine. The temperatures for injection molding of nanocomposites were set as barrel = 180–250°C, nozzle = 260°C, mold = 70°C.[8] The ABS hybrids were

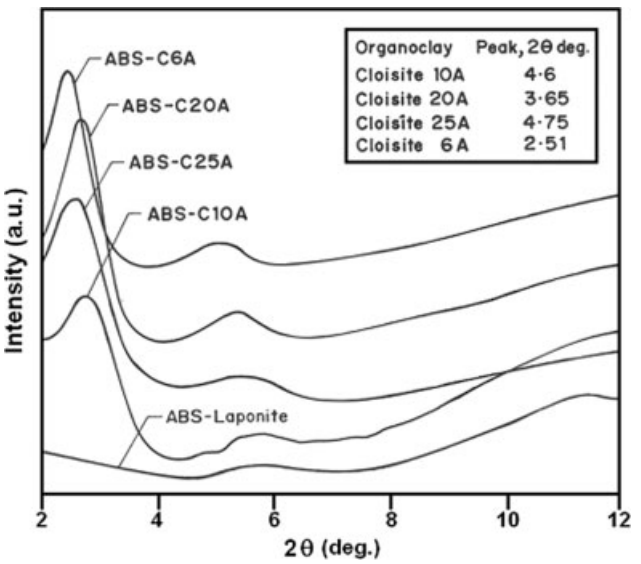

Figure 2 Combined WAXD patterns of ABS-clay hybrids prepared with various organoclays using large-scale continuous-mode twin-screw extruder.

prepared at 4 wt % organoclay loading for comparison among the different organic systems and between MMT and laponite. The standard deviation in modulus values are very satisfactory, being much less than 10% in all systems.

For the samples for studies as a function of clay loading (C20A, C25A, and laponite systems), these were prepared using the injection molding machine attached to the DSM microcompounder. The ABS hybrids were melted using the microcompounder at 190°C and 100 rpm for 5 min. The hybrid melt was then immediately injection molded with the barrel temperature set at 200°C and a mold temperature at 35°C. Tensile tests were done on a 1 kN load cell at 27°C with a constant strain rate of 5 mm/min on Instron 4204 UTM machine. Tensile data were averaged over 10 independent measurements for each nanocomposite sample and system. The data analysis was performed for each test using the software installed on the computer attached directly to the tensile tester.

Impact strength measurements were performed on notched as well as unnotched impact specimens on a CEAST impact tester at 27°C.

RESULTS AND DISCUSSION

Clay dispersion and morphology

WAXD curves in Figure 2 show clearly no exfoliation happens for MMT clays with the type of organic modifiers studied here. The d_{001} peaks for MMT-based composites and nanocomposites, observed around $2\theta \sim 2.5$–3.0°, confirm intercalation of ABS in between the clay layers for C10A, C20A, and C25A. The values of Δd_{001} are summarized in Table II. Unmodified MMT (CNa) and dioctadecyldimethyl ammonium modified MMT (C6A, with effective loading of 140 mequiv/100 g) do not lead to polymer intercalation. However, while for CNa a composite is formed, C6A leads to an unintercalated nanocomposite having good level of dispersion of the clay layers as facilitated by the dioctadecylammonium modifier. These two clays are the extreme cases, one being completely hydrophilic and other being highly hydrophobic (due to excessive organic modifier concentration). However, a decrease in the organic modifier density on MMT basal plane surface leads to polymer intercalation as observed for ABS-C20A ($\Delta d = 0.85$ nm), which contains the same type of chemical organic modifier as C6A.

The change in d_{001}-spacing (Δd_{001}) for intercalated ABS nanocomposites prepared with organoclays C20A, C10A, and C25A follows the same trend as reported earlier by Stretz et al.[27] However, the values of Δd_{001} in our study here are slightly higher (by ~ 0.3 nm) considering that L/D ratio for the screws used in our extruder is larger by a factor of 4 as compared to that used in previous study in

TABLE II
***d*-Spacing Values of Composites and Nanocomposites and Experimentally Measured Nanostructure Morphological Parameters of ABS-Clay Hybrids**

System	Hybrid *d*-spacing (nm)	Δd_{001}[a] (nm)	Second peak (nm)	FWHM, B (2θ)	N_c[b]	Particle length[c] (nm)
ABS-CNa[d]	1.27	0.06	–	1.4	8.1	185 ± 40
ABS-C6A	3.60	0.16	1.70	0.46	4.6	142 ± 16
ABS-C10A	3.15	1.23	1.52	0.73	4.0	134.7 ± 38.6
ABS-C20A	3.27	0.85	1.63	0.63	4.3	132.9 ± 28.3
ABS-C25A	3.27	1.41	1.60	0.79	4.09	128.3 ± 35.4
ABS-laponite	–	–	–	–	–	115 ± 48

[a] Difference in *d*-spacings of the nanocomposite and the clay. These results show better intercalation (0.3 nm for systems based on Cloisite 20A and Cloisite 25A) compared to those in literature.[27]
[b] Mean number of clay platelets per stack calculated using the Scherrer equation and the WAXD curves.
[c] Number-averaged value.
[d] Unmodified Na-montmorillonite.

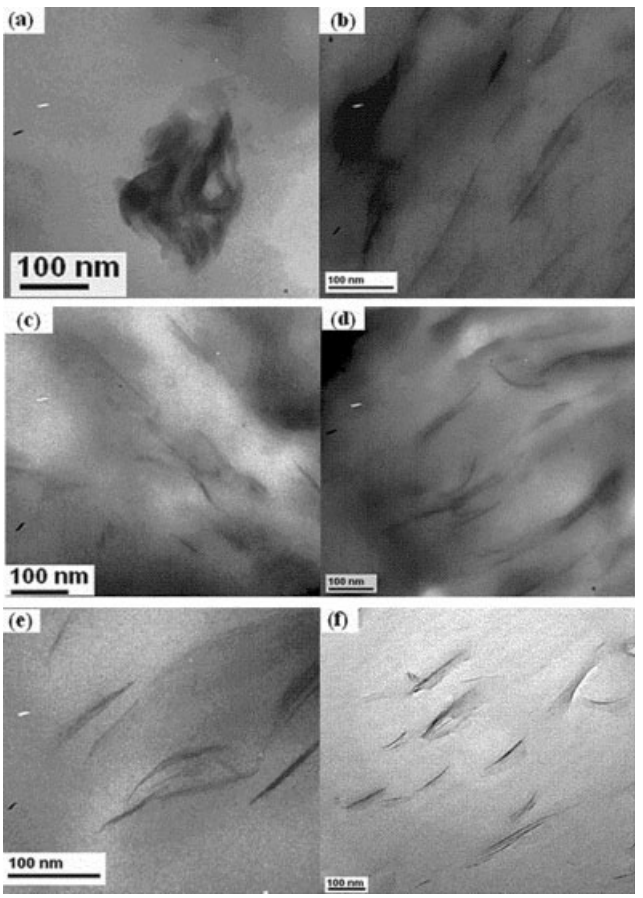

Figure 3 TEM images of ABS hybrids at 4 wt % clay. (a) ABS-CNa, (b) ABS-C6A, (c) ABS-C10A, (d) ABS-C20A, (e) ABS-C25A, and (f) ABS-laponite.

literature.[28] The use of higher L/D ratio and screw speed does not lead to degradation of ABS and organic modifier as seen from the thermal degradation stability data presented and discussed in the next section. The Δd_{001} is higher for the intercalated nanocomposites of C25A and C10A as compared to C20A. The polar acrylonitrile group in ABS matrix leads to a better molecular level interaction with the organoclays containing the dipolar benzyl moiety (C10A). The branched aliphatic group (C25A) could also be responsible for better intercalation because of favorable interaction with ABS. Although C25A is less polar as compared to C10A, the Δd_{001} for ABS-C25A nanocomposite is slightly higher by $\sim$ 0.2 nm (which is not insignificant in the context of polymer intercalation). Stretz et al.[27] have observed a difference of 0.02 nm in Δd_{001} values for ABS nanocomposites prepared with C10A and C25A. Our results for the relative trend in Δd_{001} is the same as observed previously in melt-processed nanocomposites (C25A $>$ C10A $>$ C20A) of ABS and SAN.[27] The organic modifier in C10A and C25A consists of a dominant single tallow amine (the tallow being a mixture of alkyl chains: $\sim$ 65 wt % C18; $\sim$ 30 wt % C16; $\sim$ 5 wt % C14). Therefore, this single long alkyl chain per amine molecule controls the three-way miscibility interaction between the clay framework, the organic cationic amine molecules, and the ABS segments.

The values of FWHM (which provides information on extent of clay dispersion) in Table II show that the dispersion in ABS-C25A is better than that in ABS-C10A and ABS-C20A nanocomposites. Also, Δd_{001} for these nanocomposites follows the same trend as shown by the FWHM values, clarifying that unambiguously the extent of dispersion of clay layers is better in ABS-C25A and ABS-C10A compared to ABS-C20A. Interestingly, the ABS-CNa microcomposite has higher FWHM and lower peak intensity compared to the intercalated ABS nanocomposites, a result also corroborated by the TEM images (Fig. 3).

Figure 3 clearly shows the presence of clay tactoids in the ABS-CNa system, which confirms the formation of a microcomposite. Although an unintercalated composite is formed for ABS-C6A system, it is in fact a nanocomposite due to the nanoscale thickness of the clay stacks at the levels comparable to the intercalated nanocomposites formed with C20A, C25A, and C10A organoclays. This is shown by the calculated data on number of platelets per stack (Table II). As seen in Figure 3, the intercalated clay stacks are distributed uniformly in the nanocomposite. The values of the number of clay platelets per stack are very similar in all three intercalated systems. This corroborates well with the FWHM data obtained from WAXD pattern using analysis on the basis of the Scherrer equation (differences $<$ 1 platelet/stack). The particle lengths given in Table II are the number average values for 200–250 counts for each system, except for ABS-CNa system where averaging was done using 100 counts. The number averaged particle length and number of clay particles per stack do not change appreciably with differences in chemical structure or Δd_{001} of these organoclays. Also, it is clearly found that the number of platelets per stack is slightly higher for clay particles in ABS-CNa composite system as compared to the nanocomposites.

In the case of ABS-laponite system, a small relatively wide peak appears around the clay interlayer spacing, suggesting that the system is nearly exfoliated but with few layers clearly preserving the interlamellar stacking. The TEM images in Figure 3 clearly show only one type of uniform dispersion and that there is no unintercalated region different from the rest of the sample morphology. It is clear that a nanoscale composite is formed but with few layers of laponite, which likely do not allow intercalation of ABS. For the laponite system, the statistics were obtained using 189 counts from several (nine) images to calculate the mean particle length of the

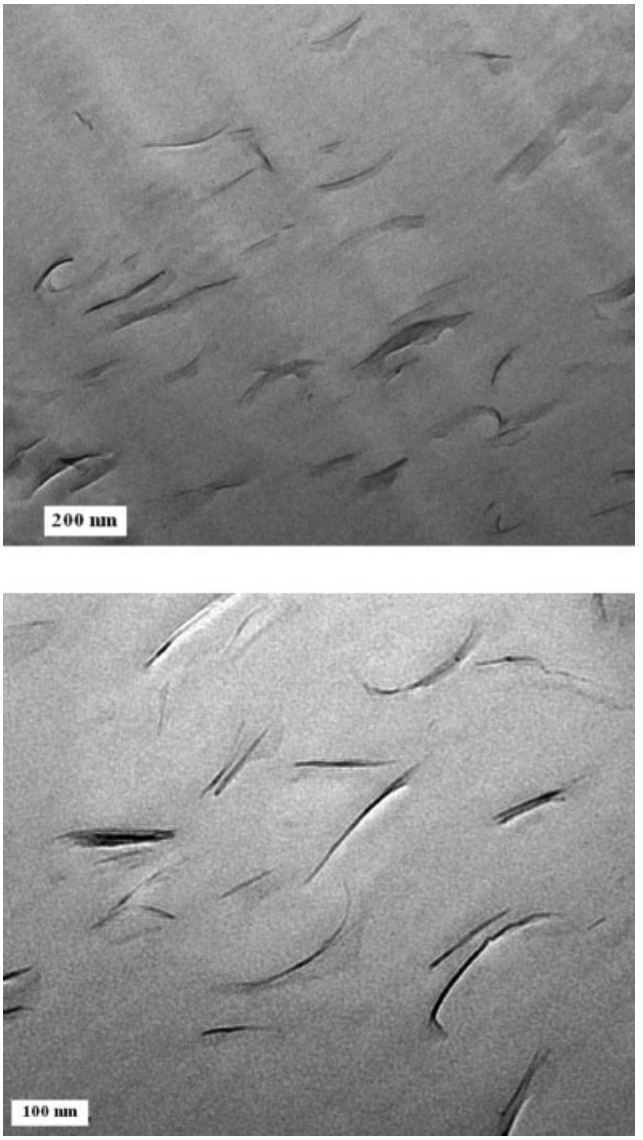

Figure 4 High-magnification HRTEM images of ABS-laponite nanocomposite at 4 wt % clay.

uniformly dispersed stacks. The laponite nanocomposite presents an interesting situation where we find that the clay particle (stack) length is higher than the length (size) of individual platelet. This is evident in the high magnification image (Fig. 4) of the high resolution transmission electron microscope (HRTEM) images. This is possible based on formation of stacks consisting of laterally shifted platelets. The NaMMT-based composite and the nanocomposites from MMT and laponite clays show clay particle sizes which are of the order of 0.1 μm, much less than those seen in other exfoliated or intercalated ABS systems (5 μm and 38 μm, respectively).[16,17]

TABLE III
Glass Transition Temperature and 5% Weight Loss Temperature of ABS-Clay Hybrids Using Large-Scale Continuous-Mode Twin-Screw Extruder

System	T_g (°C)	$T_{10\%}$ (°C)	$T_{50\%}$ (°C)
ABS	104	389	423
ABS-CNa	104	412	454
ABS-C6A	105	411	444
ABS-C10A	105	414	457
ABS-C20A	105	412	456
ABS-C25A	105	418	458
ABS-laponite	104	390	424

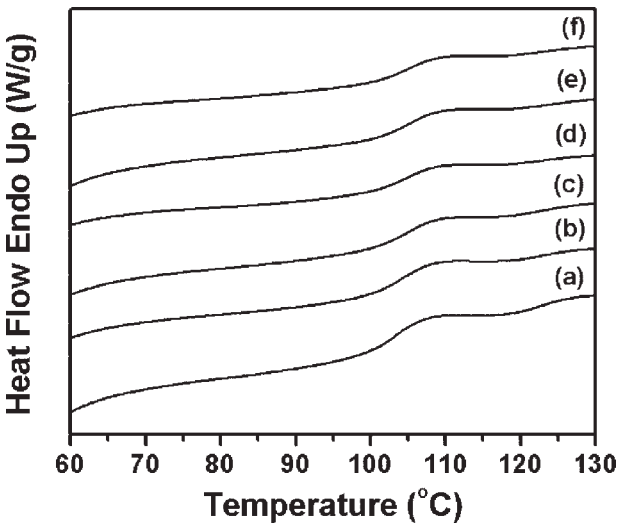

Figure 5 DSC thermographs of ABS-clay hybrids prepared at 4 wt % of organoclay loading using continuous-mode large-scale twin-screw extruder: (a) ABS, (b) ABS-CNa, (c) ABS-C6A, (d) ABS-C10A, (e) ABS-C20A, and (f) ABS-C25A.

Thermal properties of the hybrids

The T_g values of ABS hybrids as determined from DSC measurements is listed in Table III. Figure 5 shows DSC thermographs for ABS and its hybrids of 4 wt % clay content. The T_g values of ABS hybrids are unaffected by incorporation of clay at 4% loading (2.44–2.51% MMT in case of the organomontmorillonite at 4% organoclay). This is the same result whether we consider MMT or laponite clay, irrespective of the particle and platelet sizes. The transition observed for nanocomposites is mainly due to the bulk polymer as previously observed for melt-intercalated PS nanocomposites[29,30] using DSC and temperature-modulated DSC over a wide range of MMT loading. Since PS is the main component in ABS used in the present study one sees why therefore the T_g remains unaffected. Similar to the result we obtain here, previously Lee et al.,[31] having determined T_g for SAN and melt mixed SAN-organoclay (with effective loading of 140 mequiv/100 g as per C6A) nanocomposites, had observed no differences in T_g.

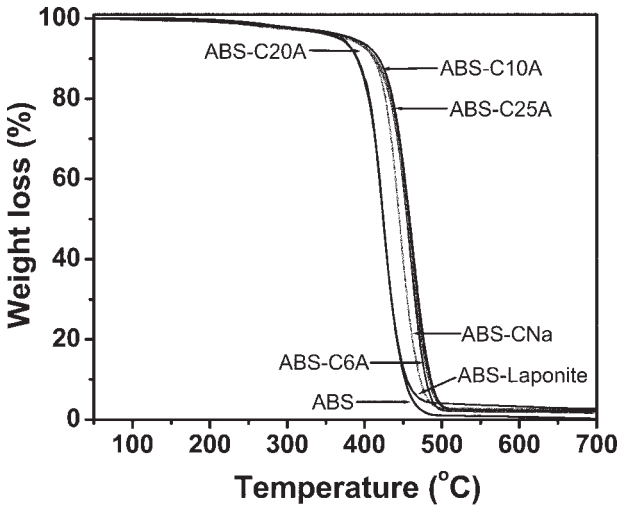

Figure 6 TGA thermographs of ABS and various ABS-clay hybrids prepared at 4 wt % of organoclay loading using continuous-mode large-scale twin-screw extruder.

The TGA overlays for ABS and its hybrids are shown in Figure 6. The temperature values at 10 and 50% wt loss for ABS and its hybrids are listed in Table III. The TGA results show an increase in 10% wt loss temperatures of hybrids by a magnitude of around 22–29°C for various hybrids, except for ABS-laponite system. The temperature at 50% wt loss shows the same trend as observed for 10% wt loss. The degradation temperature for ABS-CNa microcomposite is comparable to that of intercalated ABS nanocomposites at 10% wt loss. The char or residue for hybrids builds up on the surface of polymer during burning and reduces the rate of decomposition, improving the overall thermal stability of the nanocomposites.[16] The laponite-based nanocomposite shows the lowest improvement in the degradation stability, although the dispersion is better in these hybrids. The thermal stability of intercalated nanocomposites is found to be higher than that of ABS, because of the presence of inorganic content in the form of lamellar intercalated structure, which provides a shielding effect and increases resistance of ABS to thermal degradation.

Mechanical properties

Young's modulus (E), tensile strength at break (σ_{brk}) and % elongation at break (ε_{brk}) of the systems prepared using the larger-scale Berstoff twin-screw extruder are given in Table IV. In the case of MMT-based systems, E and σ_{brk} show significant increase at 4 wt % organoclay, while conventional microcomposite formed by unmodified CNa and the nanocomposite from excess-modified aliphatic C6A also show improvement at this level of filler. The ABS-laponite system shows a 4% improvement in modulus. The presence of clay clearly reduces the elongation at break. The increase in modulus (9.7–30%) and tensile strength (53–58%) in the systems at 4 wt % of clay (or organoclay) shows the influence of the chemical nature of the organic modifier molecule. The decrease in elongation at break is in the range of 42–72% depending on the system.

The % increase in modulus and % decrease in elongation at break for ABS nanocomposites data reported by Stretz et al.,[27] corresponding to the wt % MMT (without organic) corresponding to 4 wt % of organoclay, show an increase in modulus by 14.5%, 20% and 28.6% as compared to 22.1%, 24.4%, and 30% respectively, in our systems for nanocomposites based on C20A, C10A, and C25A. Therefore, our results are similar to earlier results on moduli for a different grade of ABS. In the present hybrids, the elongation is reduced by 61.8%, 76.5%, and 82.4% as compared to 73.8%, 73.8%, and 72.3% in their study, for C20A, C10A, and C25A nanocomposites, respectively. Nanocomposites with smaller modulus show higher values of elongation, correlating with higher ductility. Zhang et al.[26] have obtained improvement in modulus at lower clay loading ($\leq$4 wt % of clay), whereas mechanical properties have been found to be reduced at higher clay loading (>4 wt % of clay). Zheng and Wilkie[32] in their study of multicomponent blend of ABS/poly(ε-caprolactone)-Cloisite30B nanocomposites obtained exfoliated nanocomposites. However, surprisingly, in comparison with the matrix in their nanocomposite samples the values of the modulus and the stress at break (tensile strength) were lower and the elongation was higher.

Figure 7 shows the observed correlation between the Young's modulus and the change in d-spacing with various ABS-MMT hybrids studied here at 4% clay loading prepared in the large-scale Berstoff twin-screw extruder. The organoclay that leads to greater degree of intercalation gives higher improvement in the tensile modulus. Therefore, the tensile

TABLE IV
Tensile Properties of ABS-Clay Hybrids Melt Processed in Large-Scale Continuous-Mode Twin-Screw Extruder Using Unmodified and Various Organically Modified Montmorillonite Clays

System	Young's modulus, E (MPa)	Tensile strength, σ_{brk} (MPa)	% elongation-at-break (ε_{brk})
ABS	1936 ± 46	26.0 ± 9.0	13.0 ± 1.0
ABS-CNa	2124 ± 86	39.7 ± 0.6	7.5 ± 0.85
ABS-C6A	2177 ± 49	36.0 ± 1.0	4.5 ± 1.3
ABS-C10A	2409 ± 130	40.0 ± 1.9	3.4 ± 0.7
ABS-C20A	2365 ± 120	41.0 ± 3.0	3.4 ± 0.4
ABS-C25A	2512 ± 47	40.7 ± 2.0	3.6 ± 0.8
ABS-laponite	2014 ± 53	35.7 ± 1.2	3.1 ± 0.3

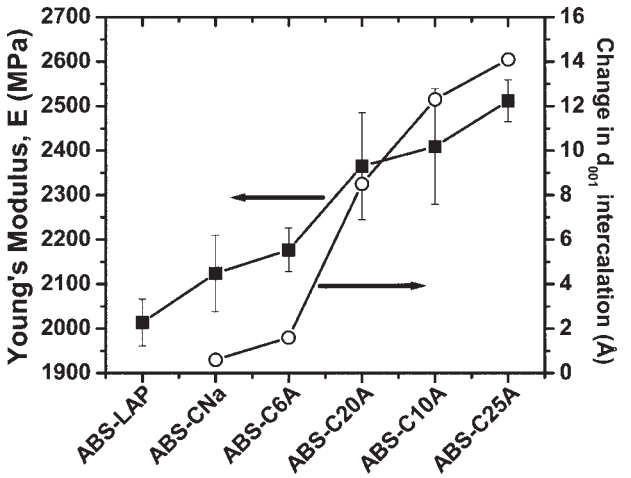

Figure 7 Variation of Young's modulus and change in *d*-spacing for various ABS-clay hybrids prepared using large-scale continuous-mode Berstoff-ZE twin-screw extruder, at 4 wt % organoclay (CNa system is without organic modification). Error bars are provided for modulus values.

modulus is higher for nanocomposite prepared with clay containing organic modifier having relatively higher polarity. Based on quantitative analysis of TEM images and data from WAXD estimation, the aspect ratio and dispersion of the clay within ABS matrix is found to not vary appreciably as a function of organic modification so as to influence the Young's modulus. However, there is a clear difference between modulus properties of unintercalated composite and that of the three intercalated nanocomposites, as arising from confinement and interactions of the intercalalated polymer chains with the silicate layers. Hybrids prepared with laponite gives a lower tensile modulus compared to those prepared with MMT. Given the result that among the intercalated nanocomposites from C25A, C20A, and C10A, the moduli are very similar (though as different levels of actual silicate filler content, at the same organoclay 4% content), we can conclude the small differences in filler content do not appreciably change the modulus.

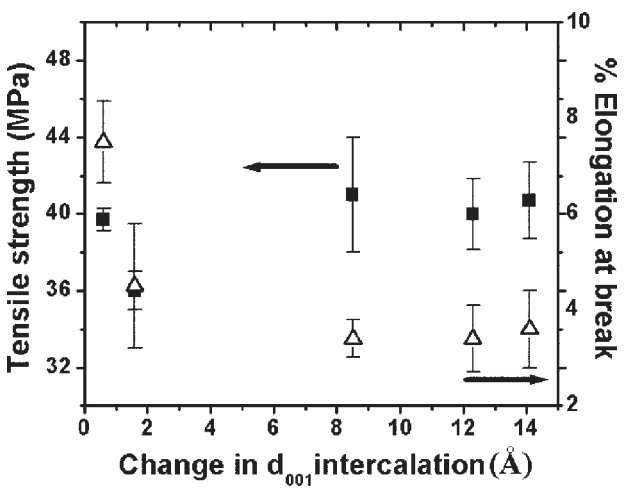

Figure 8 Variation of tensile strength and % elongation at break with change in *d*-spacing (Δd_{001}) (nm) of various hybrids based on montmorillonite, prepared using large-scale continuous-mode Berstoff-ZE twin-screw extruder at 4 wt % organoclay (CNa system is without organic modification).

TABLE V
Impact Strength of ABS-Clay Hybrids Prepared Using Unmodified and Various Organically Modified Montmorillonite Clays

Systems	Notched impact strength (J/m)	Unnotched impact strength (J/m)
ABS	135.0 ± 10.0	324.0 ± 40.0
ABS-CNa	136.0 ± 15.0	400.0 ± 30.0
ABS-C6A	173.0 ± 7.0	458.0 ± 16.0
ABS-C10A	83.0 ± 10.5	298.0 ± 11.0
ABS-C20A	74.0 ± 17.0	290.0 ± 10.5
ABS-C25A	74.5 ± 8.0	296.0 ± 19.5
ABS-laponite	106.0 ± 0.0	404.0 ± 8.0

Figure 8 shows the variation of σ_{brk} and ε_{brk} with Δd_{001}. The increase in Δd_{001} leads to a slight increase in σ_{brk}, but on the whole the strength of the nanocomposites and the composite based on unmodified MMT filler, are comparable. The tensile strength values of the nanocomposites are higher than that of ABS, contrary to what is generally observed in many cases as seen in literature in that the tensile strength of polymer–clay nanocomposite is lower than that of the polymer. Overall, there are two major significantly different levels of moduli: one level with intercalated nanocomposites and the other with the nonintercalated systems (nanocomposite and composite).

Table V shows the unnotched and notched impact strength values. Depending on the chemical structure of the organic modifier on MMT, as compared to the values of impact strength for ABS resin (matrix) the notched and unnotched impact strengths showed decrease by 38.5–45% and 20.5–22.7%, respectively, at 4% organoclay. The impact strength values are higher for ABS-CNa and ABS-C6A systems. C6A is an overexchanged organoclay, where there is increase in impact strength for both notched and unnotched specimens. We presently have no explanation for this behavior, and this would require a separate in-depth investigation. The system based on laponite clay (unmodified) at 4% loading shows better impact strength as compared to ABS, which is interesting. It could be possible due to differences in the mechanical properties of the laponite silicate layers as compared to the MMT layers.

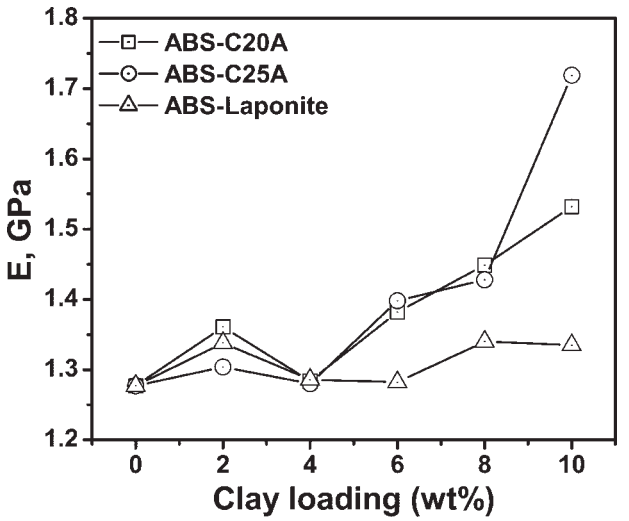

Figure 9 Effect of MMT-based organoclay loading on the layer separation (ABS intercalation) and the tensile modulus of nanocomposites.

Figure 9 shows the behavior of modulus for intercalated nanocomposites prepared with C20A and C25A as a function of MMT organoclay loading along with those of the ABS-laponite system. In the case of the branched aliphatic organic modifier in C25A, we observe no influence of filler fraction on the separation of the clay layers. In the case of the fully linear aliphatic (tallow) modifier in C20A, the extent of polymer intercalation decreases with increase in the clay fraction, possibly due to the increase in the effect of the clay–clay interlayer interactions which the polymer chains have to overcome to intercalate. The moduli and their variations are quite similar in both systems, and therefore the differences in the *d*-spacing variations do not lead to appreciable differences in the values of the mechanical modulus. Beyond 6% clay, the system based on C25A gives higher modulus at same organoclay loading because of the influence of a higher amount of MMT layer filler relative to C20A. C20A has the modifier with a higher molecular weight relative to C25A at the same organic modifier loading, which is present in both these clays (effective CEC = 95). The modulus of ABS-laponite nanocomposite does not change with clay loading. The shear during melt mixing improves the laponite platelet dispersion in ABS matrix. However, lower value of the modulus of hybrids prepared with laponite is due to the smaller size of the lateral platelet (width) dimension in case of laponite as compared to MMT. This difference between MMT and laponite-based systems gets magnified at higher clay loadings. The difference in mechanical performance even at 2% clay (modulus enhancement 20 and 35% for OMMT versus 5% for laponite at higher loading levels; while the comparison at lower loading level 2% clay showing modulus improvement 2.1% and 6.6% for OMMT versus 4.8% for laponite) is due to the significant difference in the clay platelet dimensions, likely supplemented by the difference in the modulus of the clay layers themselves. The interesting local maxima in the modulus behavior at low loading is present in all systems, this behavior is seen in prior investigations in literature in some type of polymer matrices.

CONCLUSIONS

Intercalated nanocomposites of ABS resin with layered silicates were obtained by melt state processing route. The effect of organic modifier on thermal and mechanical properties of nanocomposites has been studied in depth. The level of intercalation is comparable for nanocomposites studied previously in literature with other styrenic polymer/copolymer and same organoclays reported here. Overexchanged organoclay having fully aliphatic chemical modifier gives an unintercalated nanocomposite having same level of stack dimensions and dispersion of filler particles as compared to the intercalated nanocomposites obtained from the other organoclays. The onset of degradation for nanocomposites is higher (30–40°C) than that of ABS, depending on chemical nature of organoclay. Tensile modulus of the nanocomposites is superior to that of ABS by 4–30% depending on the type of clay. There is significant increase in tensile modulus because of formation of intercalated nanocomposites, while strain at break (elongation) significantly decreases due to the presence of clay. As compared to ABS matrix, the tensile strength of the nanocomposite is enhanced. Notched as well as unnotched impact strengths of the nanocomposites are inferior to that of ABS, following the same trend with the type of organic modification and the type of silicate. For two systems, including the ABS nanocomposite having laponite clay layers, the ductility (impact strength) is higher than that of the ABS matrix. MMT-based nanocomposites show higher moduli compared to laponite-based nanocomposites.

We are also thankful to Southern Clay Products, Inc., Texas and appreciate the generous gift of the clay samples. The authors are thankful to R. S. Gholap for transmission electron microscopy assistance. Thanks to Bayer ABS India Ltd., for the resin samples.

References

1. Giannelis, E. P. Adv Mater 1996, 8, 29.
2. Giannelis, E. P. R.; Krishnamoorti, R.; Manias, E. Adv Polym Sci 1999, 138, 107.
3. Okada, A.; Kawasumi, M.; Usuki, A.; Kojima, Y.; Kurauchi, T.; Kamigaito, O. In Polymer-Based Molecular Composites; Schaefer, D. W.; Mark, J. E., Eds.; 1990; Vol. 171, p 4; MRS Symposium Proceedings, Materials Research Society, Pittsburgh, PA, 1990.

4. Kojima, Y.; Usuki, A.; Kawasumi, M.; Okada, A.; Fukushima, Y.; Kurauchi, T.; Kamigaito, O. J Mater Res 1993, 8, 1185.
5. Fertig, R. S., III; Garnich, M. R. Compos Sci Technol 2004, 64, 2577.
6. Lan, T.; Kaviratna, P. D.; Pinnavaia, T. J Chem Mater 1994, 6, 573.
7. Gilman, J. W. Appl Clay Sci 1999, 15, 31.
8. Mark, H. F.; Bikales, N. M.; Overberger, C. G.; Menges, G. In Encyclopedia of Polymer Science and Engineering; Wiley Interscience: New York, 1986; Vol. 1, p 388.
9. Hotta, S.; Paul, D. R. Polymer 2004, 45, 7639.
10. Zhang, J.; Jiang, D. D.; Wilkie, C. A. Polym Degrad Stab 2006, 91, 641.
11. Fornes, T. D.; Yoon, P. J.; Hunter, D. L.; Keskkula, H.; Paul, D. R. Polymer 2002, 43, 5915.
12. Tiwari, R. R.; Natarajan, U. J Appl Polym Sci 2007, 105, 2433.
13. Tanoue, S.; Utracki, L. A.; Rejon, A. R.; Tatibouët, J.; Kamal, M. R. Polym Eng Sci 2005, 45, 827.
14. Yoon, P. J.; Hunter, D. L.; Paul, D. R. Polymer 2003, 44, 5323.
15. Jang, L. W.; Kang, C. M.; Lee, D. C. J Polym Sci Part B: Polym Phys 2001, 39, 719.
16. Wang, S.; Hu, Y.; Lei, S.; Wang, Z.; Chen, Z.; Fan, D. W. Polym Degrad Stab 2002, 77, 423.
17. Wang, S.; Hu, Y.; Lin, Z.; Gui, Z.; Wang, Z.; Chen, Z.; Fan, D. W. Polym Int 2003, 52, 1045.
18. Wang, S.; Hu, Y.; Zong, R.; Tang, Y.; Chen, Z.; Fan, D. W. Appl Clay Sci 2004, 25, 49.
19. Wang, S.; Hu, Y.; Wang, Z.; Yong, T.; Chen, Z.; Fan, D. W. Polym Degrad Stab 2003, 80, 157.
20. Wang, S.; Hu, Y.; You, F.; Song, L.; Chen, Z.; Fan, D. W. J Appl Polym Sci 2003, 90, 1445.
21. Zong, R.; Hu, Y.; Wang, S.; Song, L. Polym Degrad Stab 2004, 83, 423.
22. Zong, R.; Hu, Y.; Liu, N.; Wang, S.; Liao, G. Polym Adv Technol 2005, 16, 725.
23. Su, S.; Jiang, D. D.; Wilkie, C. A. Polym Degrad Stab 2004, 83, 333.
24. Su, S.; Jang, D. D.; Wilkie, C. A. Polym Degrad Stab 2004, 84, 279.
25. Zhang, J.; Jiang, D. D.; Wang, D.; Wilkie, C. A. Polym Adv Technol 2005, 16, 800.
26. Zhang, J.; Jiang, D. D.; Wilkie, C. A. Polym Degrad Stab 2006, 91, 358.
27. Stretz, H. A.; Paul, D. R.; Cassidy, P. A. Polymer 2005, 46, 3818.
28. Dennis, H. R.; Hunter, D. L.; Chang, D.; Kim, S.; White, J. L.; Cho, J. W.; Paul, D. R. Polymer 2001, 42, 9513.
29. Vaia, R. A.; Ishii, H.; Giannelis, E. P. Chem Mater 1993, 5, 1694.
30. Li, Y.; Ishida, H. Macromolecules 2005, 38, 6513.
31. Lee, S.-S.; Lee, C. S.; Kim, M.-H.; Kwak, S. Y.; Park, M.; Lim, S.; Choe, C. R.; Kim, J. J Polym Sci Part B: Polym Phys 2001, 39, 2430.
32. Zheng, X.; Wilkie, C. A. Polym Degrad Stab 2003, 82, 441.